BULLETIN OF THE POLISH ACADEMY OF SCIENCES
TECHNICAL SCIENCES, Vol. 70(6), 2022, Article number: e143537
DOI: 10.24425/bpasts.2022.143537

Interception of a hypersonic vehicle by low-speed interceptors: novel perspectives and cost optimisation

Shuangxi LIU[1], Shijun LIU[2], Binbin YAN[3]*, Tong ZHANG[1], Xu ZHANG[1], and Jie YAN[1]

[1] Unmanned System Research Institute, Northwestern Polytechnical University, Xi'an 710072, China
[2] Shanghai Aerospace Equipment Manufacturer Co., Ltd, Shanghai 200245, China
[3] School of Astronautics, Northwestern Polytechnical University, Xi'an 710072, China

Abstract. The conditions for accurately intercepting hypersonic vehicles by low-speed interceptors in the terminal guidance process are examined, considering the general form of a guidance scheme. First, based on the concept of the engagement geometry, three interception scenarios are established considering different manoeuvring configurations of the interceptors and hypersonic vehicle. Second, the boundary conditions for intercepting hypersonic vehicles (with speeds higher than those of the interceptors) are specified for the three scenarios, considering several factors: the speed, path angle, line-of-sight angle, and available overload of the interceptor; path angle and manoeuvrability of the hypersonic vehicle; and relative distance between the interceptor and vehicle. A series of simulations are performed to clarify the influence of each factor on the Interception performance in the three interception scenarios. The challenges associated with accurately intercepting hypersonic vehicles by low-speed interceptors are summarised, and several recommendations for designing guidance laws are presented.

Key words: small speed ratio; hypersonic vehicles; interception performance; boundary conditions.

1. INTRODUCTION

With rapid technological advancements, the future battlefield environment is expected to involve system-to-system confrontations [1, 2]. Moreover, in near-space scenarios, with the increasing severity of space offensive and defensive confrontations and gradual enhancement in the understanding of space resources, near-space flight vehicles have emerged as a research hotspot in various countries [3–7]. As representative near-space vehicles, hypersonic vehicles flying at Mach numbers (Ma) > 5 have broad application prospects as the likely strategic pinnacle in the future aerospace domain. Because such vehicles can realise long-distance transportation in a reasonable time, commercial applications are expected to involve high-end markets and generate significant revenues [8]. For example, the emergence of hypersonic civil flight vehicles can save the travel time of passengers, and the timely delivery of high-value items can decrease the time and cost of commercial activities. Such vehicles also have significant advantages in the military domain. The attack time of hypersonic vehicles is considerably shorter than that of low-speed flight vehicles, leading to a significantly reduced preparation and response time for defence missions and increased efficiency of mission execution. In this context, hypersonic vehicles pose a notable threat to national security, and the associated defence technologies must be researched and optimised.

Hypersonic vehicles combine the high-speed characteristics of ballistic flight vehicles with the high mobility of cruise flight vehicles, and their concealment and surprise defence capabilities surpass the target performances of the existing defence systems [9, 10]. These unique performance advantages render defence against hypersonic vehicles challenging, especially in terms of the following aspects.

1. Owing to their high flight speed, hypersonic vehicles cannot be easily detected by air defence warning systems, and their interception places higher demands on the speed and available overload of the interceptors.
2. In terms of the aerodynamic layout, hypersonic vehicles have a high lift–drag ratio and large available aerodynamic manoeuvre overload. Consequently, such vehicles can perform wave-like 'jump' manoeuvres [12,13]. The typical trajectory of a hypersonic gliding vehicle is shown in Fig. 1. The boost and inertial phases are brief, and the hypersonic vehicle attacks the target in a nearly vertical manner in the attack phase, making it difficult to intercept the hypersonic vehicle in this phase. The glide phase corresponds to a long flight time and thus a higher probability of interception suc-

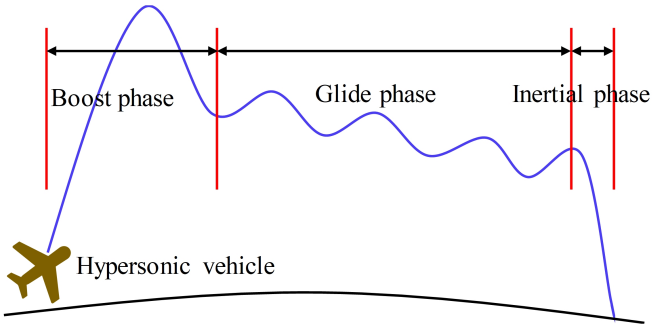

Fig. 1. Typical hypersonic gliding vehicle trajectory [11]

*e-mail: yanbinbin@nwpu.edu.cn

Manuscript submitted 2022-09-09, revised 2022-10-03, initially accepted for publication 2022-10-04, published in December 2022.

cess [14,15]. However, the high flight speeds, unpredictable trajectories, and manoeuvring uncertainties of hypersonic vehicle render interception challenging.

3. At present, interceptors typically use infrared or visible seekers [16]. However, hypersonic vehicles typically fly in the thin atmosphere, in which optical seekers encounter complex aero-optical effects: The aerodynamic heating generated by the interceptor flying at high speeds may interfere with the seeker operation, leading to aerodynamic thermal radiation and image transmission problems. Owing to these phenomena, the image on the imaging plane of the seeker may shift, vibrate, or blur [17], increasing the difficulty of target detection.

Guidance refers to the process of issuing commands for the interceptor to adjust its position and orientation to fly toward its target while satisfying several constraints [18, 19] and demonstrating the optimal performance [20, 21]. Many researchers have investigated the interception of hypersonic vehicles and designed various forms of guidance laws [22–26]. Depending on the number of interceptors, the existing guidance laws for intercepting hypersonic vehicles can be categorised as single-interceptor guidance laws or multi-interceptor cooperative guidance laws [27]. Most of the single-interceptor guidance laws are based on proportional guidance (PNG) laws, sliding mode guidance (SMC) laws, and differential game guidance laws. Kuroda *et al.* [28, 29] designed two modified PNG laws to enhance the interception accuracy of a highly manoeuvrable target with a low-speed surface-to-air interceptor. Based on the head-pursuit theory and SMC method, Zhu proposed a finite-time guidance law that could alleviate the chattering in the guidance command and increase the convergence speed and interception accuracy [30–32]. Moreover, the manoeuvrability of the hypersonic vehicle was considered in the guidance law design. Liu *et al.* [33] proposed a fractional-order fast power reaching guidance law by introducing the fractional-order operator into the sliding surface. The energy consumption associated with this guidance law was lower than that of the integral-order fast power-reaching guidance law. Considering a hypersonic multiplayer pursuit–evasion game, Liang *et al.* [34] proposed an optimal guidance scheme for the problem of the confrontation of an interceptor, a hypersonic vehicle, and an active defender.

In contrast, most of the multi-interceptor cooperative guidance laws are based on consensus protocols and area coverage strategies. Using the second-order super-twisting algorithm and a second-order consensus protocol, Liu *et al.* [35] designed a distributed cooperative guidance law to intercept hypersonic vehicles, while considering the constraints of the impact angle and interceptor speed. Moreover, based on the concepts of the interceptor reachable area, interceptor feasible area, and hypersonic vehicle escape area, a coverage-based cooperative guidance law was investigated [36], which could ensure that at least one interceptor accurately intercepts the hypersonic vehicle. This guidance law did not require any communication among the interceptors.

Notably, the abovementioned guidance laws can ensure the accurate interception of hypersonic vehicles only in certain cases. Most of the existing guidance laws have been established assuming that the flight speed of the interceptor is higher than that of the hypersonic vehicle, which places high demands on the interceptor performance and increases the combat cost. Additionally, these laws have been designed without considering the interception boundary conditions. Owing to these aspects, a given guidance law is effective only when the interceptor and its target are in a certain interception scenario. If the interception situation constraint is not satisfied, the interceptor cannot accurately intercept the target. Therefore, as discussed in this study, a comprehensive analysis of the challenges associated with the interception boundary conditions can provide a more practical and reasonable basis for the design of guidance laws.

At present, the use of low-speed and constrained manoeuvrability interceptors to intercept hypersonic vehicles represents a research hotspot [33, 35–38]. A balance must be ensured between the interception accuracy and operational economic cost when establishing defence systems against hypersonic vehicles. Thus, methods to accurately intercept hypersonic vehicles via low-cost interceptors with a low speed and constrained manoeuvrability while minimising the operational economic cost must be identified.

To address the abovementioned problems, the concept of engagement geometry is introduced to examine the problems of intercepting hypersonic vehicles using low-speed interceptors from the perspective of operational economic cost. The main contributions can be summarised as follows.

1. This study focuses on the performance of the interceptor and hypersonic vehicle, considering only a general form of the guidance scheme. The challenges associated with intercepting hypersonic vehicles via low-speed interceptors are examined, and the associated scientific problems are identified to provide reference for the design of corresponding guidance laws.
2. By comprehensively considering the speed, manoeuvring capability, and manoeuvring direction of the interceptor and hypersonic vehicle, the boundary conditions for the accurate interception of hypersonic vehicles by low-speed interceptors in different interception scenarios are specified.
3. In contrast to the existing studies [33,35–38], the conditions in which a low-cost interceptor (with a low speed and constrained manoeuvrability) can intercept a hypersonic vehicle are comprehensively analysed. By maximising the performance of low-cost interceptors in actual operational scenarios, the operational economic costs can be decreased.

The remaining paper is organised as follows: Section 2 describes the problem of a low-speed interceptor intercepting a hypersonic vehicle in the longitudinal plane. The analysis of the engagement geometry is outlined in Section 3. Details of the numerical simulations are conducted in Section 4, and the relevant discussions are presented in Section 5. Section 6 presents the concluding remarks.

2. PROBLEM DESCRIPTION

The concept of engagement geometry is introduced to analyse the boundary conditions for the head-on interception of hypersonic vehicles. The following assumptions are implemented.

Assumption 1. The influence of the Earth shape and rotation on the interceptor and hypersonic vehicle is ignored, and the entities are ideal points.

Assumption 2. The speeds of the interceptor and hypersonic vehicle remain unchanged in the engagement process.

Figure 2 illustrates the relative motion between the interceptor and hypersonic vehicle in the longitudinal plane. The nonlinear kinematic model between the interceptor and hypersonic vehicle can be expressed as

$$\begin{cases} \dot{r} = v_T \cos(\lambda - \gamma_T) - v_I \cos(\lambda - \gamma_I), \\ r\dot{\lambda} = v_I \sin(\lambda - \gamma_I) - v_T \sin(\lambda - \gamma_T), \\ \dot{\gamma}_I = a_I / v_I, \\ \dot{\gamma}_T = a_T / v_T, \end{cases} \tag{1}$$

where OXY denotes the inertial coordinate system; r denotes the relative distance between the interceptor and hypersonic vehicle; λ denotes the line-of-sight (LOS) angle; γ_I and γ_T denote the path angles of the interceptor and hypersonic vehicle, respectively; a_I and a_T denote the normal acceleration of the interceptor and hypersonic vehicle, respectively; and v_I and v_T denote the speed of the interceptor and hypersonic vehicle, respectively.

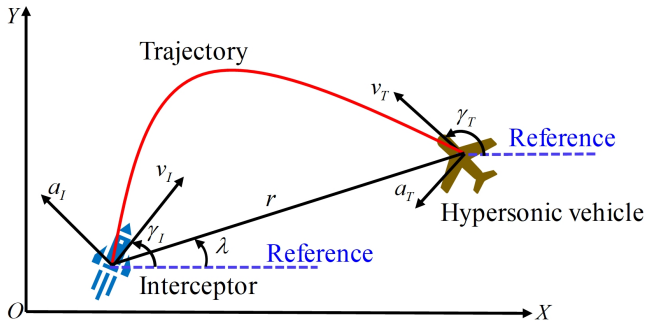

Fig. 2. Engagement process

Figure 2 shows that regardless of the movement of the interceptor and hypersonic vehicle, once the interceptor accurately intercepts the hypersonic vehicle, their displacements between the initial time and interception time form a triangle in space. This configuration is termed the engagement geometry (Fig. 3), where $\boldsymbol{s}_I$ and $\boldsymbol{s}_T$ denote the displacement of the interceptor and hypersonic vehicle in the engagement process, respectively, and A denotes the interception point in the engagement process.

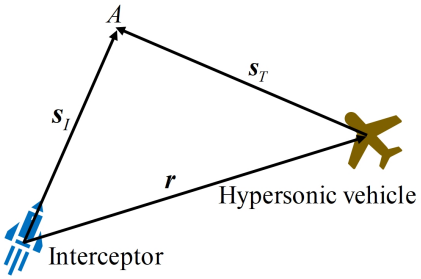

Fig. 3. Description of the engagement geometry

The ratio of the interceptor speed to hypersonic vehicle speed (hereafter, speed ratio) is defined as $\rho = \frac{v_I}{v_T}$. The research objective is to examine the variation in the engagement geometry at different speed ratios and comprehensively analyse the boundary conditions for intercepting hypersonic vehicles at different speed ratios (especially, at speed ratios < 1).

3. ENGAGEMENT GEOMETRY ANALYSIS

As shown in Fig. 3, if the interceptor accurately intercepts the hypersonic vehicle, the following expressions hold:

$$\begin{cases} \|\boldsymbol{s}_I\| = v_I t_f, \\ \|\boldsymbol{s}_T\| = v_T t_f; \end{cases} \tag{2}$$

$$\begin{cases} \|\boldsymbol{s}_I\| + \|\boldsymbol{s}_T\| > \|\boldsymbol{r}\|, \\ \|\boldsymbol{s}_I\| - \|\boldsymbol{s}_T\| < \|\boldsymbol{r}\|, \end{cases} \tag{3}$$

where t_f is the interception time.

Next, the boundary conditions for accurately intercepting the hypersonic vehicles in a head-on interception scenario are analysed in terms of the different manoeuvring configurations of interceptors and hypersonic vehicles, considering the following factors: speed, path angle, LOS angle, and available overload.

3.1. Scenario 1: The interceptor and hypersonic vehicle do not manoeuvre

If the interceptor and hypersonic vehicle do not manoeuvre during the engagement process and fly at the same altitude, the path angles of both entities remain unchanged during the engagement. The engagement geometry in this case is shown in Fig. 4.

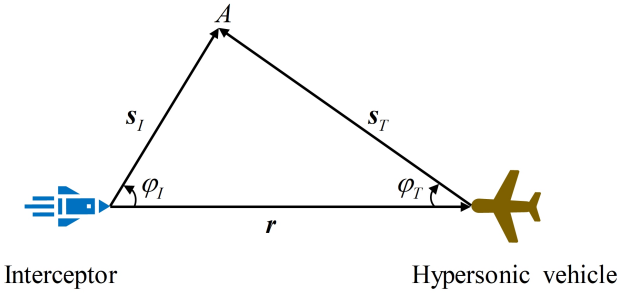

Fig. 4. Engagement geometry when the interceptor and hypersonic vehicle move at the same altitude

The sine theorem is implemented to obtain

$$\frac{\|\boldsymbol{s}_T\|}{\sin\varphi_I} = \frac{\|\boldsymbol{s}_I\|}{\sin\varphi_T} \rightarrow \frac{v_T t}{\sin\varphi_I} = \frac{v_I t}{\sin\varphi_T}. \tag{4}$$

Furthermore,

$$\frac{\sin\varphi_T}{\sin\varphi_I} = \frac{v_I}{v_T} = \rho. \tag{5}$$

For a head-on interception scenario, $\varphi_I \in (-\pi/2, \pi/2)$. Because the sign (positive or negative) of the sine function does not change within $(-\pi/2, \pi/2)$, φ_I can be expressed as

$$\cos\varphi_I = \frac{\sqrt{\rho^2 - \sin^2\varphi_T}}{\rho}, \tag{6}$$

which indicates that that when $\rho > 1$, a unique φ_I exists corresponding to φ_T. When $\rho = 1$, $\varphi_I = \varphi_T$. When $\rho < 1$, only if $\rho^2 \geq \sin^2\varphi_T$ does there exist a unique φ_I that corresponds to φ_T.

The constraint on the path angle indicates that a speed ratio smaller than 1 decreases the interceptable space for the interceptor.

3.2. Scenario 2: The interceptor manoeuvres, and the hypersonic vehicle does not manoeuvre

In this scenario, the hypersonic vehicle has a constant path angle in the engagement process. In contrast, the interceptor has an initial path angle γ_{I0} before launch. Therefore, the path angle of the interceptor must be changed to φ_I after time t_f to achieve accurate interception of the hypersonic vehicle. The corresponding engagement geometry is shown in Fig. 5.

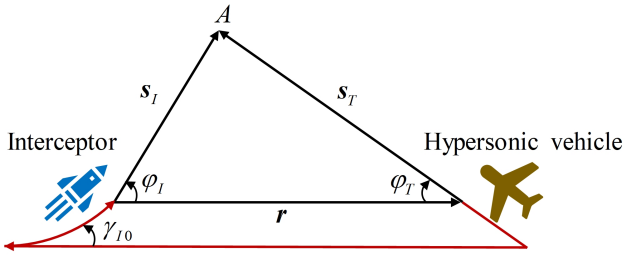

Fig. 5. Engagement geometry when the interceptor has a certain initial path angle

If the path angles of the interceptor and hypersonic vehicle in the engagement process are small, the interception time can be expressed as

$$t_f = \frac{r}{v_I + v_T}. \tag{7}$$

If the interceptor moves at its maximum available overload and is unable to redirect its speed to within the engagement geometry at time t_f, the interceptor will fail to intercept the hypersonic vehicle. To intercept the hypersonic vehicle, at least the following inequalities must be satisfied:

$$\begin{aligned} &\varphi_I \leq \gamma_{I0} + \frac{a_{I,\max}}{v_I} t_f < \frac{\pi}{2}, \\ \rightarrow\ &\varphi_I \leq \gamma_{I0} + \frac{a_{I,\max}}{v_I} \frac{r}{v_I + v_T} < \frac{\pi}{2}, \\ \rightarrow\ &\varphi_I \leq \gamma_{I0} + \frac{a_{I,\max}}{\rho v_T^2} \frac{r}{1+\rho} < \frac{\pi}{2}. \end{aligned} \tag{8}$$

Based on equation (8), the following conclusions can be derived.

1. When the speeds of the interceptor and hypersonic vehicle are certain, and the maximum available overload of the interceptor is certain, the initial path angle of the interceptor γ_{I0} has a lower limit requirement. A larger relative distance r corresponds to a smaller limit requirement for the initial path angle of the interceptor, and vice versa.
2. If the initial path angle of the interceptor γ_{I0} approaches φ_I, the available overload requirement for the interceptor is small. In contrast, if γ_{I0} differs significantly from φ_I, a larger overload is required in the engagement process.

When both the interceptor and hypersonic vehicle have a certain initial LOS angle, the engagement geometry requires a simple transformation, as shown in Fig. 6.

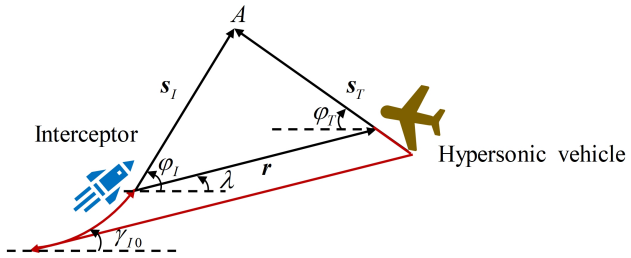

Fig. 6. Engagement geometry when the interceptor and hypersonic vehicle have an initial LOS angle

Applying the sine theorem yields

$$\frac{\|s_T\|}{\sin(\varphi_I - \lambda)} = \frac{\|s_I\|}{\sin(\varphi_T + \lambda)} \rightarrow \frac{v_T t}{\sin(\varphi_I - \lambda)} = \frac{v_I t}{\sin(\varphi_T + \lambda)}. \tag{9}$$

Furthermore,

$$\frac{\sin(\varphi_T + \lambda)}{\sin(\varphi_I - \lambda)} = \frac{v_I}{v_T} = \rho. \tag{10}$$

In this case, equation (8) can be rewritten as

$$\begin{aligned} &\varphi_I - \lambda \leq \gamma_{I0} + \frac{a_{I,\max}}{v_I} t_f < \frac{\pi}{2}, \\ \rightarrow\ &\varphi_I - \lambda \leq \gamma_{I0} + \frac{a_{I,\max}}{v_I} \frac{r}{v_I + v_T} < \frac{\pi}{2}, \\ \rightarrow\ &\varphi_I - \lambda \leq \gamma_{I0} + \frac{a_{I,\max}}{\rho v_T^2} \frac{r}{1+\rho} < \frac{\pi}{2}, \end{aligned} \tag{11}$$

which indicates that the introduction of LOS angle λ places greater demands on the initial path angle γ_{I0} and maximum available overload $a_{I,\max}$ of the interceptor.

3.3. Scenario 3: Both the interceptor and hypersonic vehicle are manoeuvring

In Scenarios 1 and 2, the hypersonic vehicle is not manoeuvring, and the speed direction is determined. Therefore, there exists only one definite interception point, and the interceptor, hypersonic vehicle, and interception point form a definite triangle. In actual engagement, however, the location of the engagement geometry is uncertain owing to the difficulty in detecting the hypersonic vehicle, errors in the identification of the speed

direction, and uncertainty regarding the manoeuvring configuration of the hypersonic vehicle. Notably, the positions of the possible engagement geometries can be determined by considering all possible speed directions of the hypersonic vehicle and obtaining the coordinates of all possible interception points based on the geometric relationships between the interceptor, hypersonic vehicle, and interception point. These positions can be used as reference for intercepting the hypersonic vehicle.

To determine the locations of all possible engagement geometries, a planar right-angle coordinate system is established in the longitudinal plane, as shown in Fig. 7.

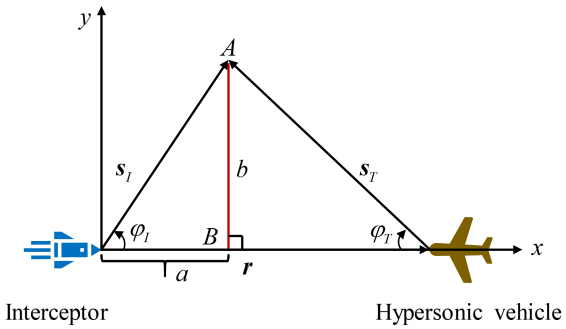

Fig. 7. Engagement geometry when the interceptor and hypersonic vehicle are manoeuvring

The origin of the coordinate system is the interceptor position. The x- and y-axes are along and perpendicular to the LOS direction, respectively. Because the speed direction of the hypersonic vehicle is uncertain, the position of interception point A is also uncertain. Notably, regardless of the interceptor and hypersonic vehicle movement, once the interceptor accurately intercepts the hypersonic vehicle, their displacements in space form a triangle. If a vertical line AB is drawn from interception point A to the x-axis (Fig. 7), two triangles can be identified. Applying the Pythagorean theorem to each of the two triangles yields

$$\|\boldsymbol{s}_I\|^2 = a^2 + b^2, \tag{12}$$

$$\|\boldsymbol{s}_T\|^2 = (r-a)^2 + b^2. \tag{13}$$

According to assumption 2,

$$\|\boldsymbol{s}_I\|^2 = \rho^2 \|\boldsymbol{s}_T\|^2. \tag{14}$$

Combining equations (12), (13), and (14) yields the following expression:

$$a^2 + b^2 = \rho^2 \left((r-a)^2 + b^2\right). \tag{15}$$

Furthermore,

$$(a - r_l)^2 + b^2 = c_l^2, \tag{16}$$

where

$$\begin{cases} r_l = \dfrac{\rho^2 r}{\rho^2 - 1}, \\ c_l = \dfrac{\rho r}{|\rho^2 - 1|}. \end{cases} \tag{17}$$

In particular, equation (16) describes the relationship between all possible interception points satisfied by the interceptor and hypersonic vehicle. The required engagement geometry is constrained and represents a circle in the considered scenario. r_l and c_l denote the transverse coordinate of the centre of the circle and radius of the engagement geometry, respectively.

Moreover, equation (16) indicates that the speed ratio ρ is a key parameter that is closely related to r_l and c_l. For a given relative distance r, r_l and c_l depend only on ρ. Therefore, the effect of ρ on the engagement geometry must be examined.

In the following analysis, r_l and c_l corresponding to $\rho < 1$, $\rho = 1$, and $\rho > 1$ are examined to obtain the mathematical expressions for the engagement geometry.

(1) $\rho < 1$

As indicated in equation (16), when $\rho < 1$, $r_l < 0$. Therefore, r_l lies on the extended relative distance r.

Moreover,

$$c_l - |r_l| = \frac{\rho r}{1+\rho} < r, \tag{18}$$

$$c_l = \frac{\rho r}{1-\rho^2} > |r_l| = \frac{\rho^2 r}{1-\rho^2}. \tag{19}$$

Thus, when $\rho < 1$, the engagement geometry surrounds the interceptor but not the hypersonic vehicle, as shown in Fig. 8.

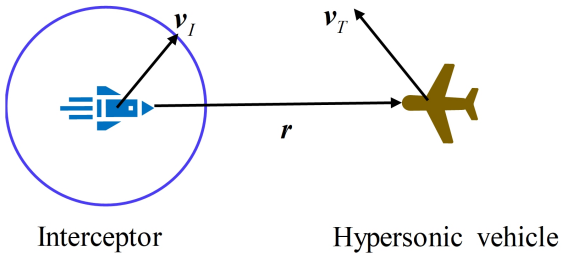

Fig. 8. Engagement geometry when $\rho < 1$

(2) $\rho = 1$

According to equation (15), when $\rho = 1$, $a \equiv \dfrac{r}{2}$, which implies that the engagement geometry a straight line, as shown in Fig. 9.

(3) $\rho > 1$

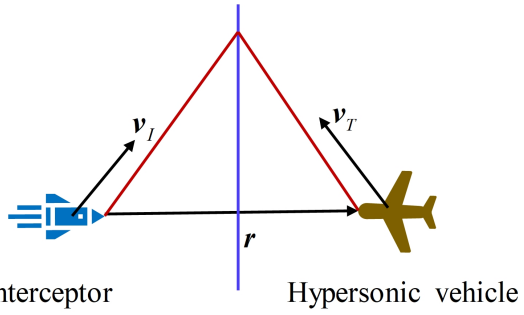

Fig. 9. Engagement geometry when $\rho = 1$

When $\rho > 1$, the following expression can be obtained considering equation (16):

$$r_l = \frac{\rho^2 r}{\rho^2 - 1} > r > 0. \tag{20}$$

In addition,

$$r_l - r = \frac{r}{\rho^2 - 1} \tag{21}$$

and

$$c_l = \frac{\rho r}{\rho^2 - 1} > \frac{r}{\rho^2 - 1} = r_l - r. \tag{22}$$

Thus, when $\rho > 1$, the engagement geometry surrounds the hypersonic vehicle but not the interceptor, as shown in Fig. 10.

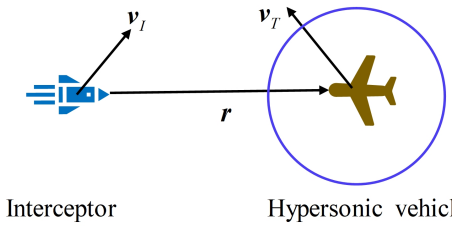

Fig. 10. Engagement geometry when $\rho > 1$

4. SIMULATION ANALYSIS

Assumption 3. The focus of this study is to analyse the interception boundary conditions between a low-speed and constrained manoeuvrability interceptor and a hypersonic vehicle. It is assumed that the interceptor can obtain the information of the hypersonic vehicle in real time.

A series of numerical simulations are performed to analyse the boundary conditions for the accurate interception of hypersonic vehicles in different interception situations (Scenarios 1–3). In all simulation cases, unless specified otherwise, the hypersonic vehicle is located at $(50, 20)$ km and flies at a speed of 6 Ma. The acceleration due to gravity is $g = 9.81$ m/s^2.

4.1. Scenario 1

According to equation (6), when the interceptor and hypersonic vehicle do not manoeuvre, the interception boundary conditions are related only to the speed ratio and path angles of the interceptor and hypersonic vehicle.

Figure 11 illustrates the relationship between φ_I and φ_T at different speed ratios. When $\rho > 1$, the interceptor only needs a small path angle to accurately intercept the hypersonic vehicle, and a larger ρ corresponds to smaller path angle required by the interceptor. When $\rho = 1$, the interception space is halved. When $\rho < 1$, the interceptor may not be able to intercept the hypersonic vehicles at all path angles, and as ρ decreases, the interceptable space of the interceptor decreases.

Next, assume that the interceptor is located at $(0, 20)$ km, the speed ratio is $\rho = 0.2, 1, 2$, and $\gamma_T = 168.5°, 135°, 90°$. The interception simulation results are shown in Fig. 12, which indicate the boundary conditions under which the interceptor can

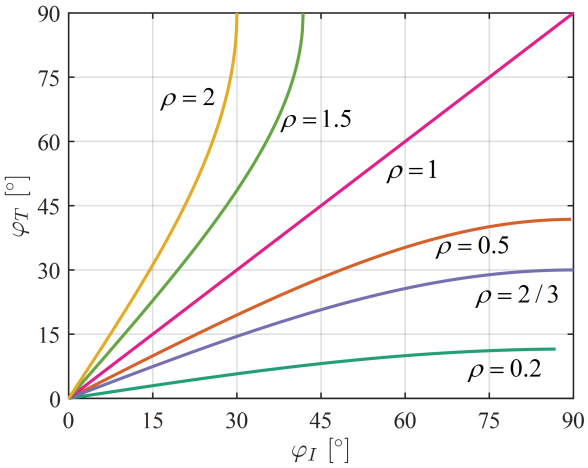

Fig. 11. Relationship between φ_I and φ_T at different speed ratios

accurately intercept the hypersonic vehicle at the three speed ratios. As shown in Fig. 12, when $\rho < 1$, the interception point must be close to the interceptor; when $\rho = 1$, the interception point must lie on the midline of r; and when $\rho > 1$, the interception point must be close to the hypersonic vehicle. In addition, when $\rho < 1$ and $\rho > 1$, the interceptor requires a larger and smaller path angle to intercept the hypersonic vehicle with a larger path angle, respectively. Furthermore, the geometric analysis shows that when $\rho = 2$, the interception area of the interceptor is 8.58% and 38.6% larger than those at $\rho = 1$ and $\rho = 0.2$, respectively. Thus, the interception performance of the interceptor deteriorates at small speed ratios.

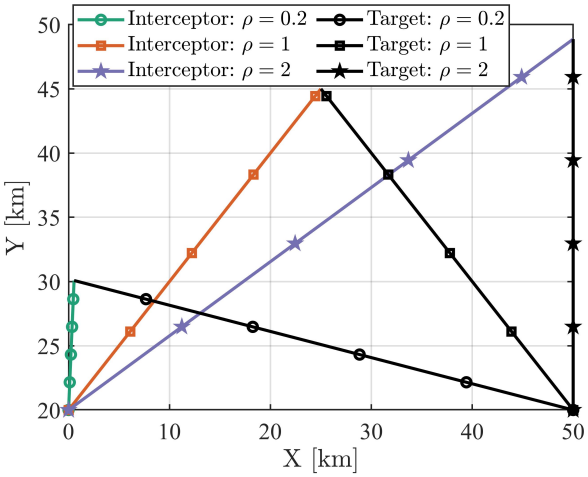

Fig. 12. Trajectories at different speed ratios

4.2. Scenario 2

The interceptor is assumed to be guided by the PNG law (23), and the effects of the speed ratio, path angle, and LOS angle on the interceptor performance are comprehensively analysed.

$$a_I = N v_I \dot{\lambda}\,. \tag{23}$$

4.2.1. Effect of the speed ratios

The interceptor is located at (0, 20) km with the maximum available overload $a_{I,\max} = 5g$. The path angles of the interceptor and hypersonic vehicle are $\gamma_I = 0.8°$ and $\gamma_T = 175°$, respectively. The speed ratio ρ varies from 0.1 to 2, and the miss distance is recorded to analyse the interception performance. The simulation results are presented in Fig. 13.

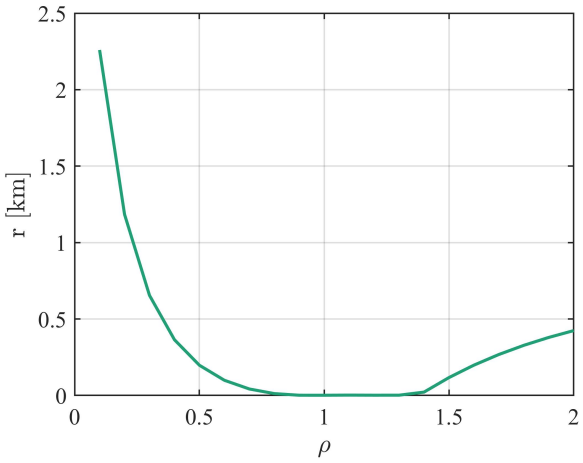

Fig. 13. Miss distance when $\gamma_T = 175°$

Figure 13 shows the influence of the interceptor speed on the interception performance is not linear, and the two parameters are not positively or negatively correlated. In certain cases, low interceptor speeds correspond to a high interception performance, and in other cases, interceptors moving at high speeds cannot successfully intercept the hypersonic vehicle.

The path angle of the hypersonic vehicle ($\gamma_T = 179°$) is modified such that the interceptor and hypersonic vehicle are in a direct head-on scenario. The speed ratio ρ is varied from 0.1 to 2 to analyse the interception performance. The simulation results are shown in Fig. 14.

Figure 14 shows that the introduced change in the path angle of the hypersonic vehicle enhances the interception performance. This finding implies that a direct head-on interception situation involves less stringent interceptor speed requirements and enhanced interceptor performance. Nevertheless, the performance enhancement is limited, and the interceptor cannot successfully intercept the hypersonic vehicles at small speed ratios.

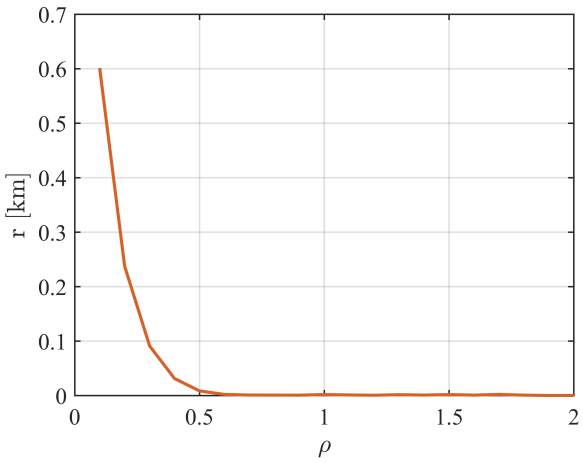

Fig. 14. Miss distance when $\gamma_T = 179°$

4.2.2. Effect of the path angles

The interceptor is located at (0, 20) km with the maximum available overload $a_{I,\max} = 5g$ and speed ratio $\rho = 2/3$. The path angle of the hypersonic vehicle, γ_T, is 175°. The path angle of the interceptor is varied from 0° to 90°, and the simulation results are presented in Fig. 15.

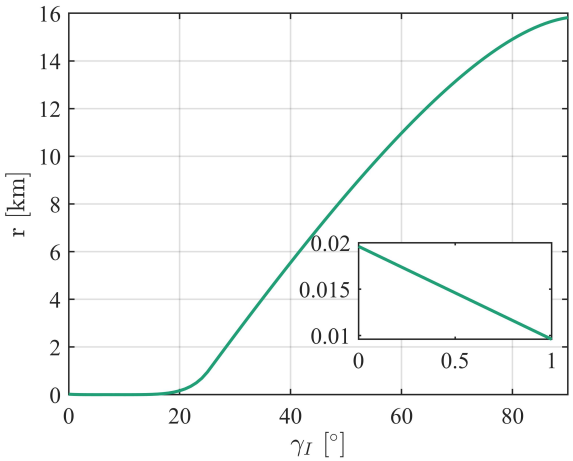

Fig. 15. Miss distance for different γ_I

Figure 15 shows that the interceptor performance deteriorates with its path angle. When the path angle of the interceptor is small (i.e., $\gamma_I < 3°$), the interception performance is low. To analyse the reasons for the degradation of the interception performance, the trajectories and guidance commands pertaining to different interceptor path angles are examined, as shown in Figs. 16–17 respectively.

The miss distances for $\gamma_I = 2°, 5°, 10°, 20°$ in the engagement process are 5.13 m, 0.22 m, 0.09 m, and 165.84 m, respectively. According to equation (8), when the initial path an-

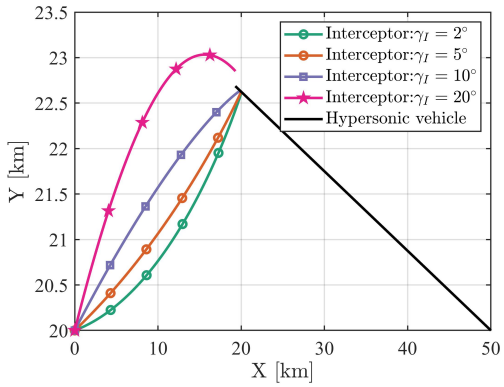

Fig. 16. Trajectories for different γ_I

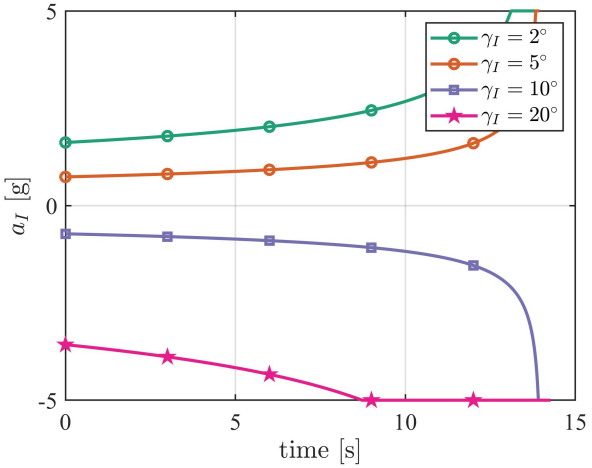

Fig. 17. Guidance commands for different γ_I

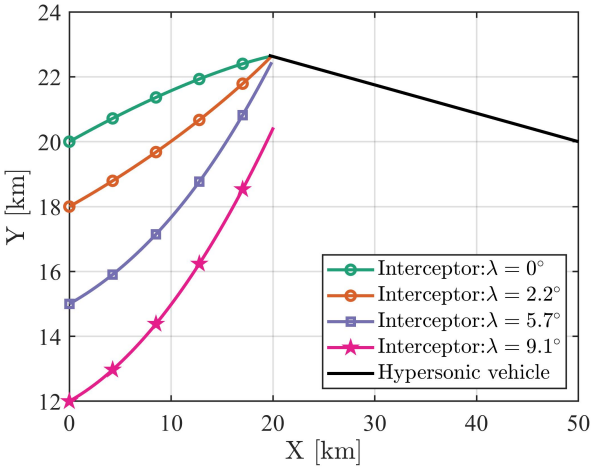

Fig. 18. Trajectories for different λ

gle is small, the interceptor must adjust this angle to meet the boundary condition of interception. Notably, the initial path angles of 2° and 20° are too small and too large to be adjusted to the desired angle φ_I at the interception time, and therefore, a large miss distance is observed for these two angles.

These findings highlight that when the interceptor and hypersonic vehicle have a certain LOS angle, the change in the initial path angle of the interceptor influences the interception performance. When the interceptor path angle approaches φ_T, the required guidance command is smaller, and in the ideal situation (head-on collision, with the hypersonic vehicle not manoeuvring) the interceptor may be able to realise uncontrolled collision. Therefore, the initial path angle of the interceptor must be as close as possible to φ_T, allowing the interceptor to intercept the hypersonic vehicle in the most efficient manner.

4.2.3. Effect of the LOS angles

The previous analyses are based on a fixed LOS angle. This subsection describes the effect of the LOS angle on the interceptor performance at small speed ratios. The simulation settings of the interceptor and hypersonic vehicle are the same as those described in Section 4.2.2. The path angle of the interceptor is set as 10°, and the interception performance is analysed for four LOS angles: 0°, 2.2°, 5.7°, 9.1°. The simulation results are presented in Figs. 18–19.

When the path angle and relative distance of the interceptor are fixed, the interception performance of the interceptor gradually deteriorates as the LOS angle increases, and the miss distances for LOS angles of $0°, 2.2°, 5.7°$, and 9.1° are $0.09m, 0.25m, 194.23m$, and $2273.57m$, respectively. This phenomenon occurs because when the LOS angle between the interceptor and hypersonic vehicle is large, the path angle of the interceptor cannot be adjusted to a suitable range even if the manoeuvre is performed with a maximum overload of $5g$, owing to the limitation of the available overload of the interceptor. Therefore, the interceptor cannot fly towards the hypersonic vehicle. This phenomenon is intensified at hypersonic speeds of approximately 6 Ma, where the interceptor must perform a large turn to intercept the vehicle.

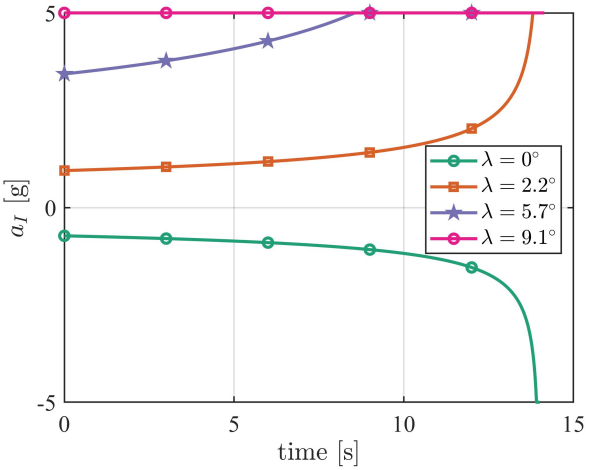

Fig. 19. Guidance commands for different λ

4.3. Scenario 3

The interceptor is assumed to be guided by the PNG law, and the hypersonic vehicle manoeuvres with a manoeuvrability of $a_T = 1g$. The effect of the available overload on the interception performance is analysed.

The interceptor is located at (0, 18) km with a path angle 10°, and the hypersonic vehicle is located at (50, 20) km with a path angle 175°. The interception performance is analysed for four interceptor available overload values: $a_{I,\max} = 5g,\ 10g,\ 15g,\ 20g$. The simulation results are presented in Figs. 20–21.

Figures 20–21 show that the interception performance is enhanced with the increase in the interceptor available overload, and the miss distances for $a_{I,\max} = 5g,\ 10g,\ 15g, 20g$ are 105.78 m, 18.17 m, 6.21 m, and 2.19 m, respectively. Therefore, if the maximum available overload of the interceptor is increased, the interceptor becomes more inclusive of the speed ratio, which enhances the interception ability. Moreover, as described in Section 4.2.2, the interception performance deteriorates when the hypersonic vehicle manoeuvres. Therefore, the

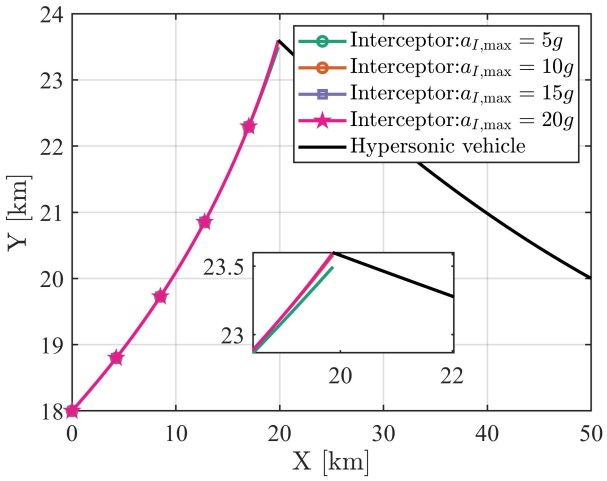

Fig. 20. Trajectories for different available overload values

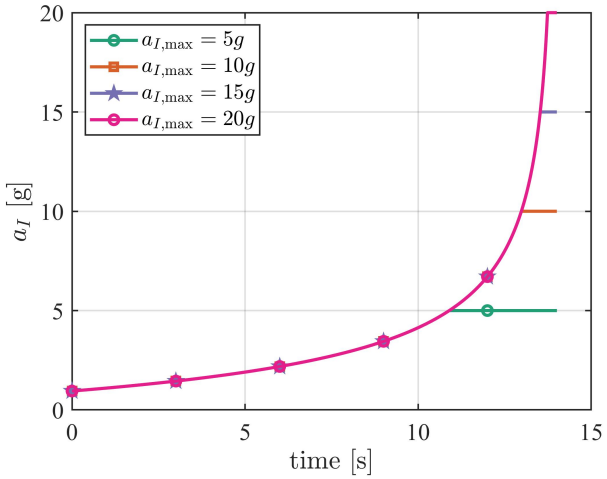

Fig. 21. Guidance commands for different available overload

manoeuvrability of the hypersonic vehicle influences the interception performance of the interceptor.

5. DISCUSSION

Based on the simulation results presented in Section 4, the following challenges can be identified for the interception of hypersonic vehicles by low-speed interceptors in the terminal guidance process:

1. Speed disadvantage: Small speed ratios result in larger relative speeds between the interceptor and hypersonic vehicle.
2. Interception situation: The path angle, LOS angle, and relative distance influence the distribution of guidance commands and thus the interception accuracy.
3. Available overload: Increasing the available overload of the interceptor can enhance the guidance accuracy of the interceptor, although this improvement may be limited by the available overload constraint of the interceptor and economic cost considerations in actual operations.
4. Manoeuvrability of hypersonic vehicles: A high manoeuvrability of hypersonic vehicles places higher demands on the initial parameters of the interceptor and available overload.
5. Guidance laws: Guidance laws can influence the flight quality of an interceptor during engagement to a certain extent, thereby influencing the interception performance. The guidance performance associated with a given guidance law is considerably influenced by the initial parameters and target characteristic. Moreover, the interception performance varies across guidance laws even under the same initial state. The guidance law and initial situation exhibit a coupled relationship.

6. CONCLUSIONS

The problems associated with the interception of a hypersonic vehicle are examined considering the ratio of the interceptor speed to the hypersonic vehicle speed. The influence of different factors (speed, path angle, LOS angle, and available overload of the interceptor; path angle and manoeuvrability of the hypersonic vehicle; and relative distance between the interceptor and vehicle) on the interception performance is examined, focusing on the scenarios in which the speed ratio is less than one. The following conclusions are derived:

1. When the interceptor and hypersonic vehicle do not manoeuvre, the boundary condition under which the interceptor accurately intercepts the hypersonic vehicle is related to the speed ratio and path angles of the interceptor and hypersonic vehicle. Smaller speed ratios correspond to higher constraints on the interceptor path angle.
2. When the interceptor manoeuvres and the hypersonic vehicle does not manoeuvre, the boundary conditions are based on the path angle and LOS angle, which are influenced by the speed ratio, available overload, and relative distance.
3. The boundary conditions for the interception of a hypersonic vehicle by a general form of the interceptor are derived for an interception scenario in which both the interceptor and hypersonic vehicle are manoeuvring. Moreover, these conditions are evaluated considering different speed ratios.

The following aspects must be considered to facilitate the interception of hypersonic vehicles by low-speed interceptors:

In an actual battlefield environment, for a given interceptor and hypersonic vehicle, the speed, available overload, and manoeuvrability are inherent properties that cannot be changed. However, the interception situation and form of the guidance law can be optimised. Therefore, the initial interception situation of the interceptor must be comprehensively considered before designing the guidance law to optimise the performance of low-cost interceptors in intercepting hypersonic vehicles in the terminal guidance process.

Future work can be focused on designing guidance laws to enable low-speed and constrained manoeuvrability interceptors to interpret hypersonic vehicles, considering the interception boundary conditions.

ACKNOWLEDGEMENTS

The authors appreciate the financial support provided by the National Natural Science Foundation of China (NSFC) (Grant No. 62173274), Natural Science Foundation of Shaanxi Province (Grant No. 2020JQ-219), Natural Science Basic Research Plan in Shaanxi Province of China (Grant No. 2020 JC-19), and Shanghai Aerospace Science and Technology Innovation Fund (Grant No. SAST2020-004).

DECLARATION OF COMPETING INTEREST

The authors declare that they have no known competing financial interests or personal relationships that could have appeared to influence the work reported in this paper.

REFERENCES

[1] Z. Xiaoying, W. Hui, M. Haihui, and W. Huaijun, "The research of digital proving ground simulation system based on hla," *Procedia Eng.*, vol. 29, pp. 3624–3630, 2012, doi: 10.1016/j.proeng.2012.01.542.

[2] X. Yu, X. Gao, L. Wang, X. Wang, Y. Ding, C. Lu, and S. Zhang, "Cooperative multi-uav task assignment in cross-regional joint operations considering ammunition inventory," *Drones*, vol. 6, no. 3, 2022, doi: 10.3390/drones6030077.

[3] F. Li, J. Xiong, X. Chen, Z. Qu, H. Bi, J. Zhang, and Q. Xi, "Near space hypersonic vehicle target tracking adaptive non-zero mean model," *IEEE Access*, vol. 10, pp. 30 445–30 456, 2021, doi: 10.1109/ACCESS.2021.3139434.

[4] K. Zhao, J. Song, S. Ai, X. Xu, and Y. Liu, "Active fault-tolerant control for near-space hypersonic vehicles," *Aerospace*, vol. 9, no. 5, p. 237, 2022, doi: 10.3390/aerospace9050237.

[5] T. Zhang, X. Yan, W. Huang, X. Che, and Z. Wang, "Multidisciplinary design optimization of a wide speed range vehicle with waveride airframe and rbcc engine," *Energy*, vol. 235, p. 121386, 2021, doi: 10.1016/j.energy.2021.121386.

[6] T. Zhang, X. Yan, W. Huang, X. Che, Z. Wang, and E. Lu, "Design and analysis of the air-breathing aircraft with the full-body wave-ride performance," *Aerosp. Sci. Technol.*, vol. 119, p. 107133, 2021, doi: 10.1016/j.ast.2021.107133.

[7] B. Xu and Z. Shi, "An overview on flight dynamics and control approaches for hypersonic vehicles," *Sci. China-Inf. Sci.*, vol. 58, no. 7, pp. 1–19, 2015, doi: 10.1007/s11432-014-5273-7.

[8] Z. Zhao, W. Huang, L. Yan, and Y. Yang, "An overview of research on wide-speed range waverider configuration," *Prog. Aeosp. Sci.*, vol. 113, p. 100606, 2020, doi: 10.1016/j.paerosci.2020.100606.

[9] Y. Lu, Z. Jia, X. Liu, and K. Lu, "Output feedback fault-tolerant control for hypersonic flight vehicles with non-affine actuator faults," *Acta Astronaut.*, vol. 193, pp. 324–337, 2022, doi: 10.1016/j.actaastro.2022.01.023.

[10] L. He, X. Yan, and S. Tang, "Spiral-diving trajectory optimization for hypersonic vehicles by second-order cone programming," *Aerosp. Sci. Technol.*, vol. 95, p. 105427, 2019, doi: 10.1016/j.ast.2019.105427.

[11] K. An, Z. Guo, W. Huang, and X. Xu, "Leap trajectory tracking control based on sliding mode theory for hypersonic gliding vehicle," *J.'Zhejiang Univ.-SCI'A*, vol. 23, no. 3, pp. 188–207, 2022, doi: 10.1631/jzus.A2100362.

[12] K. Hwang and H. Huh, "Research and development trends of a hypersonic glide vehicle (hgv)," *J. Korean Soc. Aeronaut. Space Sci.*, vol. 48, no. 9, pp. 731–743, 2020, doi: 10.5139/JKSAS.2020.48.9.731.

[13] W. Jifei, C. Jinsheng, L. Chuanzhen, D. Yanhui, and Y. Yaojie, "Aerodynamic configuration integration design of hypersonic cruise aircraft with inward-turning inlets," *Chin. J. Aeronaut.*, vol. 30, no. 4, pp. 1349–1362, 2017, doi: 10.1016/j.cja.2017.05.002.

[14] B. Cunyu, W. Peng, and T. Guojian, "Integrated method of guidance, control and morphing for hypersonic morphing vehicle in glide phase," *Chin. J. Aeronaut.*, vol. 34, no. 5, pp. 535–553, 2021, doi: 10.1016/j.cja.2020.11.009.

[15] X. Luo and J. Li, "Fuzzy dynamic characteristic model based attitude control of hypersonic vehicle in gliding phase," *Sci. China-Inf. Sci.*, vol. 54, no. 3, pp. 448–459, 2011, doi: 10.1007/s11432-011-4193-z.

[16] S. Liu, W. Liu, F. Huang, Y. Yin, B. Yan, and T. Zhang, "Multi-target allocation strategy based on adaptive sa-pso algorithm," *Aeronaut. J.*, vol. 126, no. 1300, p. 1069–1081, 2022, doi: 10.1017/aer.2021.124.

[17] D. Jing, J. CHENG, and G. Rui, "Research on near-space hypersonic weapon defense system and the key technology," *Journal of the Academy of Equipment Command & Technology*, vol. 21, no. 3, pp. 58–61, 2010, doi: 10.3783/j.issn.1673-0127.2010.03.014.

[18] X. Wang, H. Peng, S. Zhang, B. Chen, and W. Zhong, "A symplectic pseudospectral method for nonlinear optimal control problems with inequality constraints," *ISA Trans.*, vol. 68, pp. 335–352, 2017, doi: 10.1016/j.isatra.2017.02.018.

[19] W. Xinwei, L. Jie, S. Xichao, P. Haijun, Z. Xudong, and L. Chen, "A review on carrier aircraft dispatch path planning and control on deck," *Chin. J. Aeronaut.*, vol. 33, no. 12, pp. 3039–3057, 2020, doi: 10.1016/j.cja.2020.06.020.

[20] T. Han, Q. Hu, and M. Xin, "Three-dimensional approach angle guidance under varying velocity and field-of-view limit without using line-of-sight rate," *IEEE Trans. Syst. Man Cybern. -Syst.*, pp. 1–12, 2022, doi: 10.1109/TSMC.2022.3150299.

[21] T. Han, Q. Hu, H.-S. Shin, A. Tsourdos, and M. Xin, "Sensor-based robust incremental three-dimensional guidance law with terminal angle constraint," *J. Guid. Control Dyn.*, vol. 44, no. 11, pp. 2016 – 2030, 2021, doi: 10.2514/1.G006038.

[22] B. Zhao, X. Dong, Q. Li, and Z. Ren, "A combined guidance law for intercepting hypersonic large maneuvering targets," in *2020 Chinese Automation Congress (CAC)*. IEEE, 2020, pp. 1425–1430, doi: 10.1109/CAC51589.2020.9327117.

[23] C. Liu, C. Liu, and P. Tuan, "Algorithm of impact point prediction for intercepting reentry vehicles," *Def. Sci. J.*, vol. 56, no. 2, p. 129, 2006, doi: 10.14429/dsj.56.1877.

[24] Y. Si and S. Song, "Design of three-dimensional finite-time guidance law for intercepting hypersonic vehicle," *Journal of Chinese Inertial Technology*, vol. 25, no. 3, pp. 405–414, 2017, doi: 10.13695/j.cnki.12-1222/o3.2017.03.023.

[25] W. Chen, L. Shao, and H. Lei, "On-line trajectory generation of midcourse cooperative guidance for multiple interceptors," *J. Syst. Eng. Electron.*, vol. 33, no. 1, pp. 197–209, 2022, doi: 10.23919/JSEE.2022.000020.

[26] S. Wan, X. Chang, Q. Li, and J. Yan, "Suboptimal midcourse guidance with terminal-angle constraint for hypersonic target interception," *Int. J. Aerosp. Eng.*, vol. 2019, 2019, doi: 10.1155/2019/6161032.

[27] D. Qian, S. Tong, and C. Li, "Observer-based leader-following formation control of uncertain multiple agents by integral sliding mode," *Bull. Pol. Acad. Sci. Tech. Sci.*, no. 1, 2017, doi: 10.1515/bpasts-2017-0005.

[28] T. Kuroda and F. Imado, "Advanced missile guidance system against a very high speed maneuvering target," in *Guidance, Navigation and Control Conference*, 1989, p. 3445, doi: 10.2514/6.1989-3445.

[29] T. Kuroda and F. Imado, "Advanced missile guidance system against very high speed target," in *Guidance, Navigation and Control Conference*, 1988, p. 4092, doi: 10.2514/6.1988-4092.

[30] C. Zhu, "Design of finite-time guidance law based on observer and head-pursuit theory," *Proc. Inst. Mech. Eng. Part G-J. Aerosp. Eng.*, vol. 235, no. 13, pp. 1791–1802, 2021, doi: 10.1177/0954410020984562.

[31] C. Zhu and D. Mu, "Design of head-pursuit guidance law based on sliding mode control," in *IOP Conference Series: Materials Science and Engineering*, vol. 563, no. 4. IOP Publishing, 2019, p. 042076, doi: 10.1088/1757-899X/563/4/042076.

[32] C. Zhu and Z. Guo, "Design of head-pursuit guidance law based on backstepping sliding mode control," *Int. J. Aerosp. Eng.*, vol. 2019, 2019, doi: 10.1155/2019/8214042.

[33] S. Liu, B. Yan, X. Zhang, W. Liu, and J. Yan, "Fractional-order sliding mode guidance law for intercepting hypersonic vehicles," *Aerospace*, vol. 9, no. 2, p. 53, 2022, doi: 10.3390/aerospace9020053.

[34] H. Liang, Z. Li, J. Wu, Y. Zheng, H. Chu, and J. Wang, "Optimal guidance laws for a hypersonic multiplayer pursuit-evasion game based on a differential game strategy," *Aerospace*, vol. 9, no. 2, p. 97, 2022, doi: 10.3390/aerospace9020097.

[35] S. Liu, B. Yan, R. Liu, P. Dai, J. Yan, and G. Xin, "Cooperative guidance law for intercepting a hypersonic target with impact angle constraint," *Aeronaut. J.*, vol. 126, no. 1300, pp. 1026–1044, 2022, doi: 10.1017/aer.2021.117.

[36] S. Liu, B. Yan, T. Zhang, X. Zhang, and J. Yan, "Coverage-based cooperative guidance law for intercepting hypersonic vehicles with overload constraint," *Aerosp. Sci. Technol.*, vol. 126, p. 107651, 2022, doi: 10.1016/j.ast.2022.107651.

[37] S. Liu, Y. Wang, Y. Li, B. Yan, and T. Zhang, "Cooperative guidance for active defence based on line-of-sight constraint under a low-speed ratio," *Aeronaut. J.*, p. 1–19, 2022, doi: 10.1017/aer.2022.62.

[38] S. Liu, B. Yan, T. Zhang, P. Dai, R. Liu, and J. Yan, "Three-dimensional cooperative guidance law for intercepting hypersonic targets," *Aerosp. Sci. Technol.*, vol. 129, p. 107815, 2022, doi: 10.1016/j.ast.2022.107815.